Raman light scattering from supracritical binary fluid mixtures: CH4/CF4

F. G. Baglin, S. Sweitzer, and W. Stanbery

Citation: The Journal of Chemical Physics **105**, 7285 (1996); doi: 10.1063/1.472599
View online: http://dx.doi.org/10.1063/1.472599
View Table of Contents: http://scitation.aip.org/content/aip/journal/jcp/105/17?ver=pdfcov
Published by the AIP Publishing

Raman light scattering from supracritical binary fluid mixtures: CH_4/CF_4

F. G. Baglin, S. Sweitzer, and W. Stanbery
Chemical Physics Program/216, University of Nevada, Reno, Nevada 89557-0020

(Received 7 December 1994; accepted 31 July 1996)

A supracritical fluid mixture of CH_4/CF_4 (1:9 mole ratio) has been studied at 323 K at densities between 3.0 and 19.1 mol -✓ (m/✓) by inelastic (Raman) light scattering originating from the ν_1 totally symmetric stretching mode of methane. Furthermore, a Raman depolarization ratio study of the integrated intensities of the ν_1 mode was also carried out as a function of density. A model is proposed to aid in the understanding of the intensity-density behavior in terms of both allowed and interaction-induced (ii) contributions to the overall observed signal. The model makes use of one, two, and three body light scattering via both the dipole polarizability, the dipole–quadrupole polarizability, and also takes into account various partner combinations in the multibody light scattering. Whereas, the model generally predicts correct $I_{\nu h}$ behavior, (here I is the Raman intensity and the subscripts refer to the vertical polarization direction of the laser (ν) and the direction of the analyzer either ν or h (horizontal)), it is shown that the standard assumption of the no $V-R$ coupling is violated, leading to a different mechanism for $I_{\rm iso}$ Raman light scattering. This leads to extensive three-body ii $I_{\rm iso}$ signal cancellation, but none from the $I_{\nu h}$ spectrum. The model adequately explains these concepts through the usual interaction induced processes as well as a unique cross term. © *1996 American Institute of Physics.* [S0021-9606(96)52441-4]

I. INTRODUCTION

Over the past 30 years the coincident fields of interaction-induced, ii, spectroscopy via absorption and light scattering have become well established as arising from non-equilibrium fluctuations in density. Indeed, this spectroscopy has enriched the literature to the point that a complete review in this paper is not possible. However, we begin by giving two reviews that cover the work from the seventies and early eighties through 1994.[1,2] We now limit the references given to those of direct interest to this paper, in particular, the early work of LeDuff and co-workers[3–6] on tetrahedral species as well as the work of many others[7–35] on associated systems. Generally speaking, the work has focused on single component systems at densities (d) below $d_{\rm crit}$ (for example, in pure CH_4 $d_{\rm crit}=6.091\times10^{21}$ molecule/cc or 10.1 m/✓) and temperatures above $T_{\rm crit}$. However, in order to better understand the fundamental mechanisms of supracritical extraction and solvation, it is necessary to be able to monitor solute–solvent interactions at a fundamental level. Thus the thrust of this current paper is to observe, via Raman light scattering (RLS), ii phenomena over a wide density range using equations of state, both measured and developed, as a guide. As will be seen, there are many unexpected results (unexpected meaning in contrast to our understanding of RLS at both lower densities as well as from single component systems). We have chosen to use a monitor, or probe, molecule that has an allowed I_{vv} signal, i.e., the totally symmetrical v_1 mode of CH_4 and its forbidden I_{vh} signal (more specifically v means the z or vertical laser polarization direction and h means the x or horizontal direction; moreover the RLS tensor is symmetric so $xz=z$ and $xy=yx$ for the traceless components).

The I_{vv} signal is related to the I_{vh} signal by a relationship which will be fully explained and used later, but is well-known, i.e.,

$$I_{\rm iso}=I_{vv}-4/3(I_{vh}). \tag{1}$$

Here, $I_{\rm iso}$ has only the trace terms from the RLS tensor of CH_4 and due to CH_4's T_d symmetry the trace terms yield a scalar i.e. tensor rank, $l=0$ (hence isotropic scattering). The I_{vh} or—anisotropic RLS, yields data on the orientational properties ($l=2$) of the probe and here is nonzero because of ''ordinary'' two-molecular dipole polarizability dipole–induced-dipole (DID) ii RLS as well as two-molecule dipole–quadrupole polarizability RLS. This latter mechanism arises from the field gradient present between two molecules i.e. a field gradient induced dipole, or FGID, process. In general, the DID process dominates ii spectra, e.g., in Ref. 3 most of the RLS from the CF_4/Ar arises from DID, but LeDuff *et al.* also noted that neglected effects such as higher multipole interactions (meaning primarily FGID or other short-range interactions) contribute significantly to the ii of the two-body CF_4–Ar.

Beyond the experimental results, many workers[3,12–15,17] have proposed models for the origin of the observed RLS ii spectra over the years. Before proceeding to the next section we also wish to explicitly mention the contribution of Posch[15] to the field of ii light scattering mechanisms, particularly for Rayleigh scattering and Madden[18] for his early models and insight into ii processes. Both groups were very early to model scattering terms at intermediate to high density in Rayleigh (Posch) and Raman (Madden) light scattering for tetrahedral molecules.

Lastly, the focus of this paper is directed to three main points, (1) How is is possible that the $I_{\rm iso}$ ii contributions are so large in comparison to the $I_{vh}=I_{\rm aniso}$ signals? (2) Are the Raman depolarization ratios (RDR) useful in tracking the scattering mechanism (i.e., DID or FGID) as shown by

Posch[15] for the Rayleigh scattering and also found by Hacura, Yoon, and Baglin for the forbidden v_2 band of CO_2?[19] and, (3) How is it possible for so much detail to be seen in the I/d vs d spectra given in the figures of this paper when one monitors a vibrational signal at 2915 cm^{-1}, i.e., far removed from the solvent or bath energies? This question presupposes that we realize that we are monitoring translational and/or reorientational coordinates when we observed the ii contributions to I_{vv}, $I_{\rm iso}$, or I_{vh}. Furthermore, one might wonder about the origin of the structure in I/d vs d data. This will also be discussed.

We now proceed to Sec. II, Theory, where we will develop a model based upon results of Ladanyi,[20] Sec. III, Experiment, where details of the measurements are given, Sec. IV, Results, wherein the figures are present, Sec. V, Discussion, where several aspects of the model and the results seen in the figures will be brought together in three subsections and last, Sec. VI, Conclusions.

II. THEORY

Below is the model proposed by Ladanyi[20] for RLS for the symmetric stretching mode of a tetrahedral molecule, CH_4. Whilst the model does not present new concepts, it is specialized to the particular mode (v_1) of our probe system and includes explicitly the involvement of the solvent (CF_4) system; these together make it very insightful.

We will present the model, comment upon some of the unusual assumptions, made, and then point out some of those which will be important later in the discussion section. It is relevant to note now, however, that the Coriolis coupling concept is not explicitly covered in the model (hereafter the BL model) nor in any other model with which we are familiar, but this coupling plays a key role in utilizing the model.

The total induced dipole for a collection of molecules is given by

$$\mathbf{M}=\Pi\cdot\mathbf{E}, \tag{2}$$

where Π is the polarizability and $\mathbf{E}$ the applied field. In general, Π contains contributions from single molecules and from interactions involving pairs, triplets, etc., of molecules. If we consider only the first order ii terms, we get for tetrahedral molecules

$$\Pi=\Sigma_i\alpha_i\mathbf{I}+\Sigma_i\Sigma_{j\neq i}[\alpha_i\alpha_j\mathbf{T}_{ij}+\tfrac{1}{3}\alpha_j\mathbf{A}_i:\mathbf{T}_{ij}^{(3)} -\tfrac{1}{3}\alpha_i\mathbf{T}_{ij}:\mathbf{A}_j+\cdots], \tag{3}$$

where we have explicitly included the following interactions: Dipole–induced dipole (DID) and two types of dipole–quadrupole (DQ) interactions: in one the field gradient in molecule j induces a dipole in molecule i and in the other the field from molecule i induces a quadrupole in molecule j. In Eq. (3), $\mathbf{I}$ is the unit dyadic, $\mathbf{T}_{ij}$ the dipole tensor, $\mathbf{T}_{ij}^{(3)}$ the dipole–quadrupole interaction tensor, α_i the ordinary (dipole) polarizability and $\mathbf{A}_i$ the dipole–quadrupole polarizability tensor, which depends on molecular orientation.[21,22]

The Raman polarizability is obtained by differentiating the molecular polarizabilities and $\mathbf{A}_i$ appearing in Eq. (3) with respect to the appropriate vibrational coordinate (q_i) of molecule i. In the case of the symmetric stretch mode, the resulting polarizability derivatives, and, have the same symmetry as the original molecular polarizabilities. For this mode, we find

$$\begin{aligned}\pi_i' q_i&=\left(\frac{\partial\pi}{\partial q_i}\right)_{q_i=0} q_i\\ &=\{\alpha_i'\mathbf{I}+\Sigma_{j\neq i}[2\alpha_i'\alpha_j\mathbf{T}_{ij}\\ &\quad+\tfrac{2}{3}\alpha_i'\mathbf{T}_{ij}^{(3)}:\mathbf{A}_j-\tfrac{2}{3}\alpha_j\mathbf{A}_i':\mathbf{T}_{ij}^{(3)}]\}q_i\end{aligned} \tag{4}$$

and the Raman polarizability is

$$\Pi_{\rm RAM}=\Sigma_i\pi_i' q_i=\Sigma_i[\alpha_i'\mathbf{I}+\Sigma_{j\neq i}\Delta\pi_{ij}']q_i, \tag{5}$$

where $\Delta\pi_{ij}'$ is the interaction-induced polarizability derivative given by the term in square brackets in Eq. (4).

The polarized and depolarized Raman intensities are obtained by averaging, respectively, the squares of a diagonal (for example, zz) and an off-diagonal (for example, xz) component of $\Pi_{\rm RAM}$. Since vibrational coordinates of different molecules can, to a good approximation, be taken as uncorrelated, this corresponds to

$$I_{vv}\cong\Sigma_i\langle(\pi_i'^{zz})^2q_i^2\rangle \quad\text{and}\quad I_{vh}\cong\Sigma_i\langle(\pi_i'^{xz})^2q_i^2\rangle. \tag{6}$$

As has been shown in the context of Rayleigh scattering,[22] $\Delta\pi_{ij}'$ for tetrahedral molecules can be separated into isotropic ($\ell=0$), and anisotropic ($\ell=2$) components

$$(\Delta\pi_{ij}'^{\alpha\beta})_0=\tfrac{2}{3}(\alpha_i'\mathbf{T}_{ij}^{(3)}:\mathbf{A}_j-\alpha_j\mathbf{A}_i':\mathbf{T}_{ij}^{(3)})_0^{\alpha\alpha}\delta\alpha\beta \tag{7}$$

and

$$(\Delta\pi_{ij}'^{\alpha\beta})_2=2\alpha_i'\alpha_jT_{ij}^{\alpha\beta}+\tfrac{2}{3}(\alpha_i'\mathbf{T}_{ij}^{(3)}:\mathbf{A}_j-\alpha_j\mathbf{A}_i'\mathbf{T}_{ij}^{(3)})_2^{\alpha\beta}, \tag{8}$$

where the Cartesian components are given by α and β and the subscripts denote tensorial rank. The second rank component contributes to anisotropic scattering and has the property

$$\langle(\Delta\pi_{ij}'^{zz})_2^2\rangle=\tfrac{4}{3}\langle(\Delta\pi_{ij}'^{xz})^2\rangle. \tag{9}$$

The subscript 2 has been omitted from the right-hand side of Eq. (9) since off-diagonal components have entirely $\ell=2$ character. Eq. (9) allows us to obtain the isotropic intensity from Eq. (6) as given earlier, i.e.,

$$I_{\rm iso}=I_{vv}-\tfrac{4}{3}I_{vh}. \tag{10}$$

We see from Eq. (7) that the DID mechanism does not contribute at first order to isotropic scattering from tetrahedral molecules, but that the DQ mechanism does. Furthermore, since α_i' is isotropic, I_{vh} is purely interaction-induced, while I_{vv} and $I_{\rm iso}$ are not. Specifically,

$$I_{vh}=\Sigma_i\langle q_i^2\Sigma_{j\neq i}\Delta\pi_{ij}'^{xz}\Sigma_{k\neq i}\Delta\pi_{ik}'^{xz}\rangle \tag{11}$$

and

$$I_{\rm iso}=\Sigma_i\{\langle(q_i\alpha_i')^2\rangle+2\Sigma_{j\neq i}\langle q_i^2\alpha_i'(\Delta\pi_{ij}'^{zz})_0\rangle +\Sigma_{j\neq i}\Sigma_{k\neq i}\langle q_i^2(\Delta\pi_{ij}'^{zz})_0(\Delta\pi_{ik}'^{zz})_0\rangle\}. \tag{12}$$

Equation (12) contains a cross term between molecular and induced polarizabilities. This term would vanish under the assumption, made in theories of Rayleigh scattering from tetrahedral molecules,[21,22] that intermolecular pair correlations are independent of molecular orientations. This approximation is not made here, since the presence of this term might account for the observation that $I_{\rm iso}/d$ (d=density) is strongly density dependent for methane-perfluoromethane mixtures. Another approximation usually made for Raman scattering is that vibrational coordinates are uncorrelated from rotational and translational coordinates. Equations (11) and (12) do not include this approximation, since it is not clear that it is valid for the systems considered here with Coriolis coupling (second order) in ν_1 of CH_4.

Equations (11) and (12) are valid for one-component systems as well as mixtures of tetrahedral molecules. In the case of a binary mixture, the sums and the values given to the polarizabilities can be interpreted to correspond to the particular situation considered. For example, for a mixture containing N_M molecules of methane and N_F molecules of perflouromethane in which methane is the scatterer, we can write

$$I_{vh}=I_{vh}^{(2)}(M,M)+I_{vh}^{(2)}(M,F)+I_{vh}^{(3)}(M,M,M)+I_{vh}^{(3)}(M,M,F)+I_{vh}^{(3)}(M,F,F) \tag{13}$$

and

$$I_{\rm iso}=I_{\rm iso}^{(1)}(M)+I_{\rm iso}^{(2)}(M,M)+I_{\rm iso}^{(2)}(M,F)+I_{\rm iso}^{(3)}(M,M,M)+I_{\rm iso}^{(3)}(M,M,F)+I_{\rm iso}^{(3)}(M,F,F), \tag{14}$$

where the superscripts indicate how many molecules are involved and the terms in the brackets denote the species that contribute. For example,

$$I_{\rm iso}^{(1)}(M)=N_M(\alpha'_M)^2\langle q_1^2\rangle, \tag{15}$$

$$I_{\rm iso}^{(2)}(M,M)=N_M(N_M-1)[2\alpha'_M\langle[\Delta\pi'^{zz}_{12}(M,M)]_0q_1^2\rangle+\langle[\Delta\pi'^{zz}_{12}(M,M)]_0^2q_1^2\rangle], \tag{16}$$

$$I_{\rm iso}^{(2)}(M,F)=N_MN_F[2\alpha'_M\langle[\Delta\pi'^{zz}_{12}(M,F)]_0q_1^2\rangle+\langle[\Delta\pi'^{zz}_{12}(M,F)]_0^2q_1^2\rangle], \tag{17}$$

$$I_{\rm iso}^{(3)}(M,M,M)=N_M(N_M-1)(N_M-2)\times\langle[\Delta\pi'^{zz}_{12}(M,M)]_0[\Delta\pi'^{zz}_{13}(M,M)]_0q_1^2\rangle, \tag{18}$$

$$I_{\rm iso}^{(3)}(M,M,F)=2N_M(N_M-1)N_F\langle[\Delta\pi'^{zz}_{12}(M,M)]_0\times[\Delta\pi'^{zz}_{13}(M,F)]_0q_1^2\rangle, \tag{19}$$

and

$$I_{\rm iso}^{(3)}(M,F,F)=N_MN_F(N_F-1)\times\langle[\Delta\pi'^{zz}_{12}(M,F)]_0[\Delta\pi'^{zz}_{13}(M,F)]_0q_1^2\rangle. \tag{20}$$

Similarly,

$$I_{vh}^{(2)}(M,M)=N_M(N_M-1)\langle[\Delta\pi'^{zz}_{12}(M,M)]^2q_1^2\rangle, \tag{21}$$

$$I_{vh}^{(2)}(M,F)=N_MN_F\langle[\Delta\pi'^{zz}_{12}(M,F)]^2q_1^2\rangle, \tag{22}$$

$$I_{vh}^{(3)}(M,M,M)=N_M(N_M-1)(N_M-2)\times\langle\Delta\pi'^{xz}_{12}(M,M)\Delta\pi'^{xz}_{13}(M,M)q_1^2\rangle, \tag{23}$$

$$I_{vh}^{(3)}(M,M,F)=2N_M(N_M-1)N_F\times\langle\Delta\pi'^{xz}_{12}(M,M)\Delta\pi'^{xz}_{13}(M,F)q_1^2\rangle, \tag{24}$$

and

$$I_{vh}^{(3)}(M,F,F)=N_MN_F(N_F-1)N_F\times\langle\Delta\pi'^{xz}_{12}(M,F)\Delta\pi'^{xz}_{13}(M,F)q_1^2\rangle. \tag{25}$$

The terms in the polarized intensity I_{vv} can be obtained by substituting Eqs. (15)–(25) into Eq. (10).

To conclude the theory section, it is important to enumerate the assumptions that are of particular importance to interpretations to be offered later. There are three assumptions which will play a significant role in the data interpretation, (1) vibrational coordinates on different molecules are uncorrelated (the notable exception shown by among others Doege and Yarwood[23] is vibrational resonance exchange from Raman signals that have a very strong infrared intensity counter-part) and (2), vibrational coordinates are not correlated with translational and rotational coordinates and (3), intermolecular pair correlations are independent of molecular orientations. Only assumption (1) is found in Eq. (6) and is included in those following it. The inclusion of vibrational–reorientational–translational correlation has been examined in several models,[24–27] but a truly detailed examination seems lacking. Moreover, experimentally, no cleancut examples have been found in condensed phases. Note that in this BL model the $V-R$ correlation is included to give rise to a crossterm in Eq. (12).

III. EXPERIMENT

The sample mixture was prepared by AGA specialty gases of Maurnee, Ohio at the 1:9 ratio as has been done for all of the other systems studied. The data were again recorded on our Jobin–Yvon 1 m U-1000 Raman system and the high pressure system described elsewhere.[6,11] All data were taken at 323 K with an estimated error of ± 0.5 K and the pressure-density data came from the N.I.S.T. program library using an extended corresponding states algorithm with standard correlated shape factors and 1,1,1,2-tetrafluoroethane as the reference fluid.[28] The uncertainties associated with the calculation are 3%. The PVT calculations compared very well in the ambient to 400 atm. range reported by Douslin, Harrison, and Moore.[29] Most errors occurred near the critical density of the CF_4 which we carefully avoided in our experiments. All data were gathered at 2 cm^{-1} slits (200 μ) and were checked against results obtained at 100 μ slits and no difference was found in any of the Raman depolarization ratios (RDR). No signal intensity was observed beyond $W_0 \pm 10$ cm^{-1} (where W_0 is the signal center). Thus unlike in Rayleigh scattering results, the measurable wings from Raman scattering are greatly reduced in

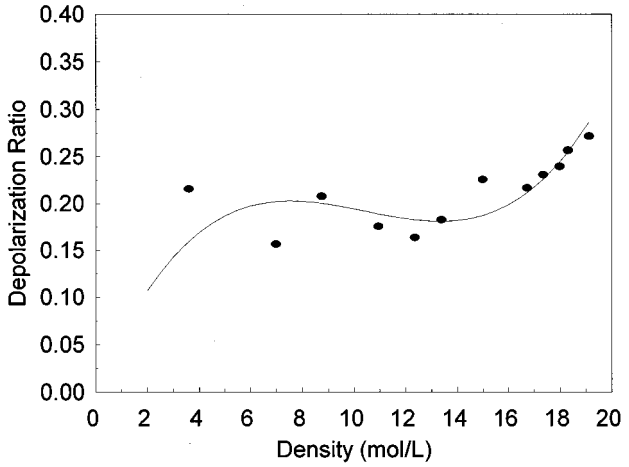

FIG. 1. Raman depolarization ratio (RDR) for 1:9 CH_4/CF_4 between 3 and 19 m/l at 323 K. Line fit is $RDR=6.64\times10^{-2}d-6.89\times10^{-3}d^2+2.2\times10^{-4}d^3$ ($d\equiv$density in m/l).

intensity and therefore analysis beyond a few cm^{-1} from W_0 was too difficult due to slow S/N in the signal's wings. This is particular true for solution studies. We attempted to use much narrower slits but even after extensive signal averaging (30 scans) no additional information was forthcoming as the S/N was still too weak and no time scale separation was possible. We also used the more conventional procedure of opening the monochromator slits; also to no avail.

We estimate the error in the light scattering data below 10 m/ℓ to be at most 15% (10% is more realistic) and above 10 m/ℓ 10% (5% is more realistic) above 10 m/ℓ for both I_{iso} and I_{aniso} data. Finally, we collected a 8.67 h scan of $I_{\nu h}$ with 2 cm^{-1} slits and again no additional ''wing intensity'' could be found over a 50 cm^{-1} window either side of 2915 cm^{-1} (W_0).

Using data collected from the known RDR for the 1→3 rotational transition of H_2 (RDR=0.75), we have been able to correct our pressure RDR values from 10–1000 bars. This corrected data is given in Fig. 1. Moreover, relative Raman differential scattering cross-sections for $I_{\nu\nu}$ of ν_1 were also measured at 35.50 and 68 bars and yielded $3.74\times10-30$ cm^2/sr molecule (they gave a 0.06% precision and fall between a 4.9% error and a 0.00% error compared to all literature value). Although more detailed cross section results will be given in a later publication, we simply wish to clearly establish that our experimental setup is more than adequate for precise, as well as accurate measurements of RDR and intensity results.

IV. RESULTS

Figure 1 shows the RDR results from the ν_1 symmetric stretching frequency in CH_4, Figs. 2 and 3 show, respectively, the logarithms of the isotropic and anisotropic intensities vs wave numbers from the ν_1 signal center at 3.6, 7.0, 13.4, and 16.8 m/ℓ (which correspond to pressures of 80, 150, 500, and 1120 bars), Figs. 4 and 5 show the I_{iso}/d and I_{aniso}/d vs density respectively. Figure 6 shows the RDR as a function of frequency shifts ($W-W_0$), near the ν_1 frequency at the indicated densities.

We observed that the RDR data in Fig. 1 didn't display a maximum as the pure methane RDR data had.[7] Indeed, this

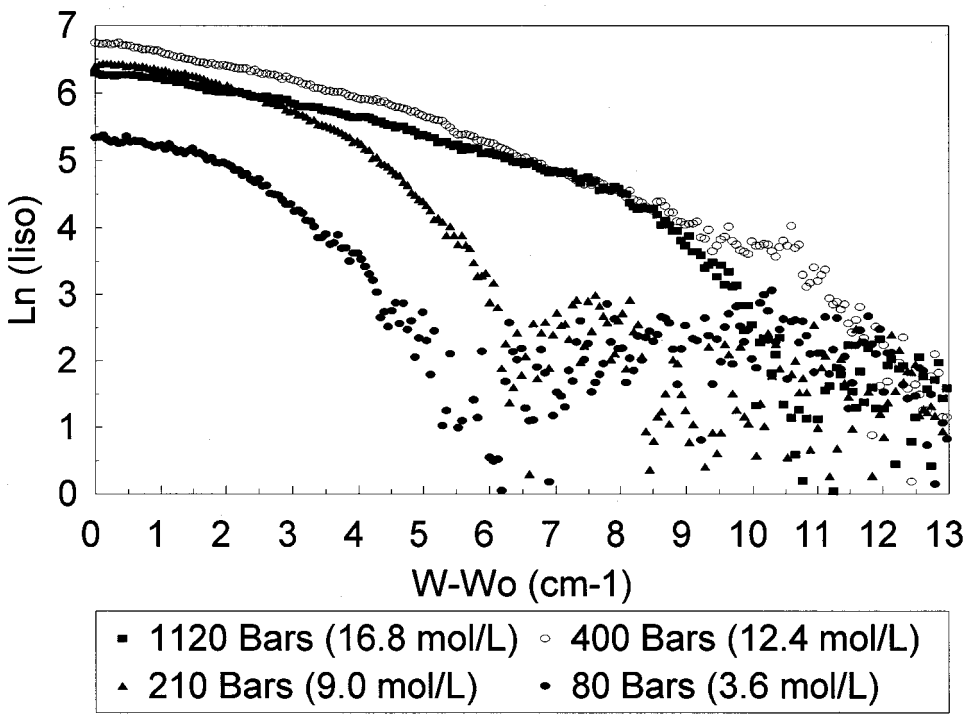

FIG. 2. Logarithm of the isotropic intensity (I_{iso}) as a function of frequency displacement from the signal maximum at W_0. The lower intensity portion at each indicated pressure (density) is the background noise.

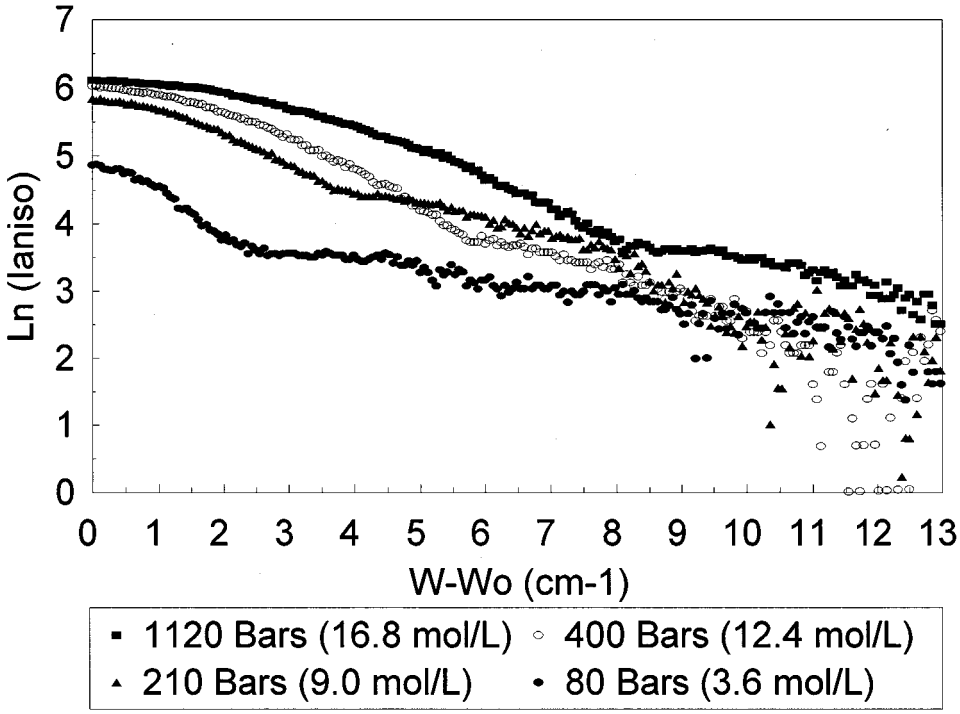

FIG. 3. Logarithm of the anisotropic intensity ($I_{\text{aniso}}-I_{vh}$) as a function of frequency displacement from the signed maximum at W_0. The lower intensity portion at each indicated pressure (density) is the background noise.)

maximum resulted directly from the fact that the I_{vv} from pure CH_4 increases in an approximately linear fashion with density as expected for electric dipole allowed processes (a more detailed dependence will be the subject of a future paper). Therefore, we were quite surprised to find that only the isotropic data showed spectral intensity cancellation (most often referred to as three-body cancellation). The anisotropic cancellation was dramatically altered (eliminated) compared with pure CH_4 results. In the mixture this effect led directly to the linear increase in the RDR values with

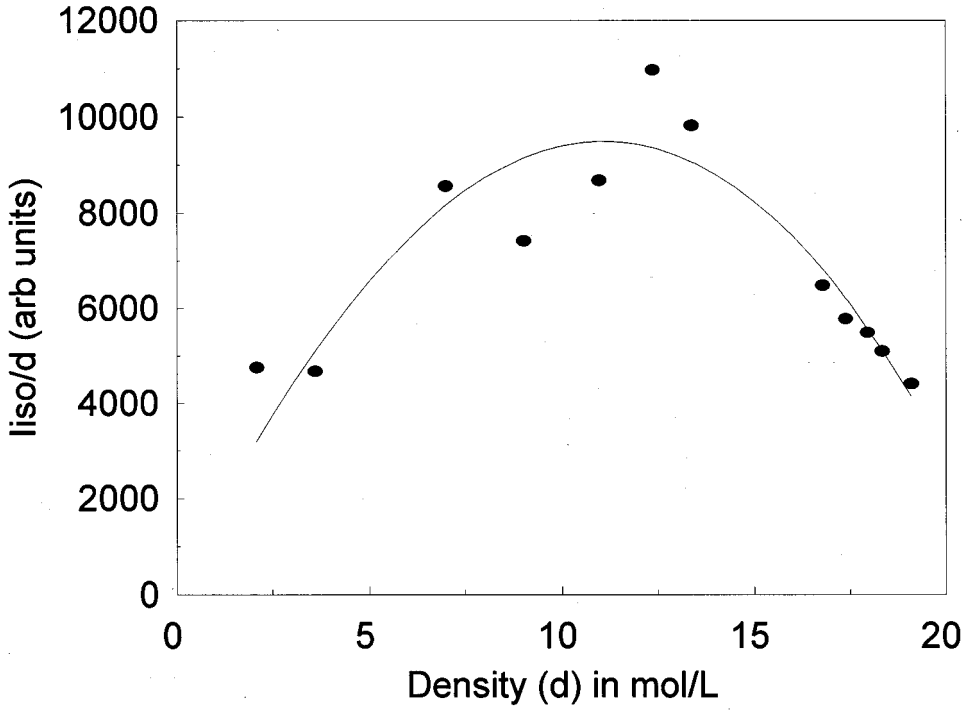

FIG. 4. I_{iso}/d vs d (density in m/**l**) between 3 and 19 m/**l**. The line represents a fit of I_{iso}/d (d) i.e., $I_{\text{iso}}/d=1672d-70d^2-0.33d^3$.

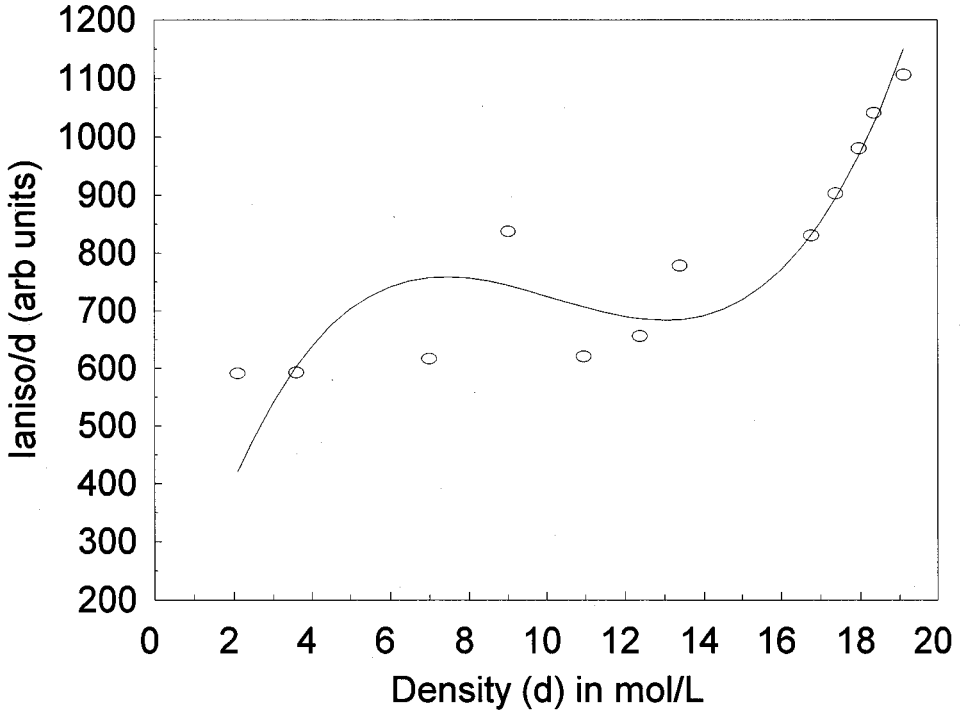

FIG. 5. I_{aniso}/d vs d between 3 and 19 m/**l**. The line represents a fit of I_{aniso}/d (d), i.e., $I_{\text{aniso}}/d = 252d - 27d^2 + 0.87d^3$.

density due to the significant cancellation in the RDR denominator (I_{vv}). This cancellation result can also be seen more clearly from the data in Fig. 4. This result is not completely unprecedented as Thibeau, Tabisz, Oksengorn, and Vodar[30] observed such behavior in Ar gas and CH_4 gas at elevated densities in a series of Rayleigh scattering experiments in 1970. In addition, the Rayleigh work of several authors summarized by Madden in 1991[18] also indicates this possibility. That the cancellation is so much less in the I_{aniso} date here in the mixture (Fig. 5) than in pure methane was

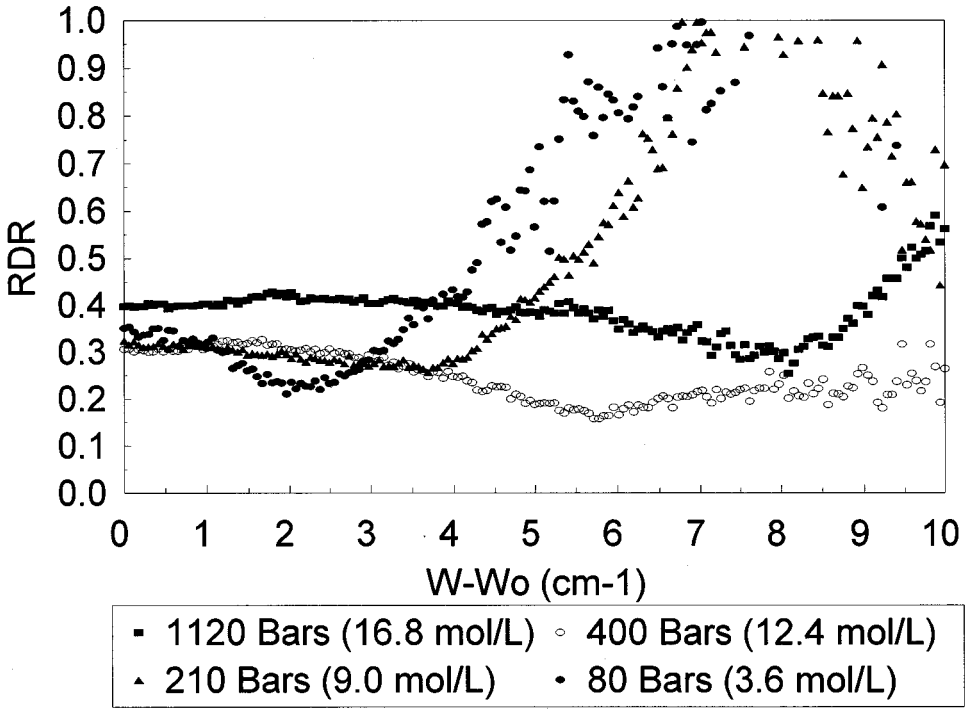

FIG. 6. Raman depolarization ratio values as a function of frequency shift $(W - W_0)$ from the signal maximum at W_0. The pressures (densities) are indicated.

predicted earlier by Friedrich, Tarjus, and Kivelson.[31] We have been unable to document previous I_{iso} Raman intensity cancellation behavior by other workers. It should be mentioned that we examined three other data sets (different, but similar densities) and all showed this remarkable result. In Fig. 2, we note that the noise in the spectral wings is simply due to the weakness of the signal.

The lines found in Figs. 1, 4, and 5 are all fits to a general equation of the form $I/d=ad+bd^2+cd^3$. Thus I/d (here I is the I_{iso} or $I_{aniso}=I_{\nu h}$ intensity) is fit to a function cubic in the system density and in Figs. 1 and 5 the line would extrapolate to zero density. However, in Fig. 4 the line extrapolates to a constant value characteristic of the allowed signal's scattering cross section. Each figure caption contains the values for a, b, and c.

V. DISCUSSION

The BL model as presented here gives all the pertinent RLS scattering mechanisms and includes only one of the earlier mentioned three assumptions, i.e., no (or very little) vibrational phase correlation between neighboring molecules. We believe that since the model allows for vibration–rotation correlation this has a direct bearing on the objectives (1) and (3) found at the end of Sec. I. Specifically, objectives (1) and (3) involve the ii part of the ln I_{iso} and ln I_{aniso} (Figs. 2 and 3) and with the structure of I_{iso}/d and I_{aniso}/d vs d (Figs. 4 and 5). So we must examine, in detail, the mechanism leading to Eq. (12) of the BL model.

Once we complete this introductory section of the discussion, we will proceed to Sec. V A—a discussion of Figs. 2 and 3, then to Sec. V B—a discussion of Figs. 4 and 5 then to Sec. V C–a discussion of Figs. 1 and 6. In connection with the latter section, we note that Posch[15] has given a method via Rayleigh depolarization ratios to determine the predominant ii scattering mechanism (e.g., DID or FGID). Lastly, we note again that other workers[19] have used the same procedure in RLS RDR for a forbidden signal to obtain similar results (i.e., 3/4 for DID and 9/37 for FGID). We will address the question of whether this procedure is appropriate for a signal whose $I_{\nu\nu}$ signal is allowed and whose $I_{\nu h}$ signal is forbidden.

A. The signal intensities for I_{iso} and I_{aniso}

In order to find the explanation for the large I_{iso}/d (or simply the isotropic intensities) we return first to Eq. (12). Once this discussion is finished we then comment on the BL model's treatment of I_{aniso}. The discussion following Eq. (12) shows clearly that only the allowed [(i.e., first term in Eq. (14))] should be strong, but it would be constant in the I_{iso}/d vs d plots; moreover, the last term is FGID in origin and cannot possibly give rise to an ii signal of the observed magnitude.

However, we note that the time scales for vibrational dephasing and the ii process are essentially identical.[17] Indeed, we have the allowed breathing mode correlated with a reorientational ii term in Eq. (12), i.e., the middle term. For such correlation to exist through this cross term, there must be a coupling term between these energetically different processes. So, how does the ν_1 vibration couple to the rotational degrees of freedom when the bath temperature is 323 K equivalent to 225 cm^{-1}, and ν_1 is near 2915 cm^{-1}? Many years ago, Nakagawa and Shimanouchi[32] observed first and second order Coriolis ($V-R$) coupling in methane. In particular, the first order coupling coefficient is 5.0 cm^{-1} (which couples the E type bending modes to overall rotation) and a second order coefficient equal to a value between 0.5 and 0.8 cm^{-1} which couples the A_1, ν_1, mode to overall rotation. Here, the actual values of the coupling coefficients were found by Lolk and Robiette[33] in the calculation of the vibrational potential energy surface between 2600 and 3300 cm^{-1} for methane. The 5 cm^{-1} is about ten times the size of usual first order coriolis coupling coefficients. Therefore, the second order coefficients in methane is about the size of most observed first order constants. This was pointed out several years ago by us in our first work on pure methane.[7] This established how the 225 cm^{-1} bath modes couples to the ν_1 mode near 2915 cm^{-1}.

Once the $V-R$ intramolecular coupling has been established then coupling to translation coordinates could also be possible. Moreover, as noted above, the allowed ν_1 component is involved in Eq. (12) and would therefore supply most of the intensity to this electric dipole allowed ii cross term which is coupled via the second order Coriolis coefficient to the solvent (bath) coordinates. It is also noteworthy that both Doege and Yarwood[34] and Van Woerkom, DeBlejser, DeZwart, and Leyte[35] have shown that vibrational relaxation due to intermolecular interactions depends upon the reorientational behavior of molecules in the liquid. They also show that generally such correlations of V and R will not occur in I_{iso} signals; however, here we have an unusual situation i.e., second d order (A_1 via F_1 to the heat bath) Coriolis coupling.

The BL model's Eqs. (11) and (13) show DID for the two-body and FGID for the two-body intensities in Eqs. (21–25). Specifically, and finally are the DID (α') terms and FGID ($\mathbf{A}'$ terms) respectively. Note that unlike I_{iso} or I_{vv}, all of these terms are of ii origin and have been discussed in detail by other workers[21,22] and by us in the theory section. We discuss the lack of cancellation in the next section.

B. The shapes of $I_{\nu\nu}/d$ and $I_{\nu h}/d$ vs density and three-body cancellation

Even a cursory examination of Figs. 4 and 5 show that at high densities the signal I_{iso}/d is drastically reduced from earlier densities; whereas in $I_{\nu h}/d$ there is no cancellation present. It is surprising that this occurs, but only if one insists that the isotropic and anisotropic signal cancellation processes arise from the same mechanism. The BL model gives a clue to the origin of the problem; perhaps Eq. (12) illustrates it best for $\ell=0$, i.e., I_{iso}/d data. Note that the $\ell=0$ data incorporates the vibrational coordinates into the intensity expression for I_{iso}, i.e., within the correlation functions. Note also that this expression exists in the anisotropic data in Eq. (11). In contrast to this in I_{iso}/d, the cancellation is occurring because as Schweitzer and Chandler[27] point out,

''*the general behavior of the vibrational coordinates is for them to lose phase memory as the density increased* ⋯.'' Indeed, Fig. 4 clearly shows that behavior and hence I_{iso}/d vs d shows cancellation a dephasing effects. At the same time in the anisotropic RLS, Bratos,[24] Bratos and Tarjus[26] and Tarjus, Kivelson, and Friedrich[35] have made a strong case that mixed systems (solute–solvent systems as we have here) are *not* expected to display cancellation to any significant degree, since the three-body cancellation terms are large negated by the presence of solvent around the solute.

The $I_{\nu h}/d$ vs d data seen in Fig. 3 ln (I_{aniso}) vs $W-W_0$ (W_0 is the frequency of the signal maxima and W is some other higher frequency value) reveals the increasing intensity of the anisotropic RLS at higher densities. It is important to recall that, in contrast to I_{iso}, the I_{aniso} arise only from DID terms. How can this be understood via Eq. (23) and (25) that describe three-body signal cancellation? We appeal here to,[18,35] our model equations and a simple adaptation of the lattice gas model. Let us begin with the lattice gas model. Consider a two-dimensional model (directly extendable to three-dimensions) of methane (M) and tetrafluoromethane (F). Then using an equilateral triangle as a high density template of instantaneous position of M,M,M in Eq. (20); M,M and F in Eq. (21) and M,F,F, in Eq. (22) we find the following respective symmetries: M,M,M-D_{3h} and M,M,F, or M,F,F,-C_{2V}. As Refs. 36 and 18 have shown, the lower symmetry reduces $I_{\nu h}$ signal cancellation. In Fig. 3 we can see a regular increase in $\ln(I_{aniso})$ vs $(W-W_0)$ from 3.6 to 16.8 m/ℓ; contrasting sharply to the Fig. 2 results. This behavior is also seen most clearly in Figs. 4 and 5. Although our two-dimensional equilateral triangle model is crude, we can adapt the lattice gas models as Ref. 31 did and one can show for a two-dimensional model that $(N/L)^L$=probability of three-body cancellation. Here, L is the number of lattice sites (3) and N is the number of CH_4 (probe) molecules on the three sites. We then find respectively for $N=3$, 2 or 1, $P_3=1$ [Eq. 20], $P_2=0.3$ [Eq. 21] and $P_1=0.027$ [Eq. 22]. Whereas this example is over simplified, there is no need to complicate a straight forward principle; as the density increases, the number of CF_4's around methane also increase and little cancellation occurs. Only if solute aggregation (or sometimes called augmentation) increases should three-body cancellation be expected to be significant. We have, therefore, shown generally the increase and the decrease in I_{iso}/d vs d and the steady increase with density in I_{aniso}/d vs d can be explained as long as one does not insist that the mechanisms for RLS I_{iso} and RLS I_{aniso} must be the same. It is not clear whether there is any two molecule phase correlation from this data (the assumption associated with Eqn. (6)), but it is very clear that $V-R$ coupling via the second order Coriolis constant completely alters the expected isotropic RLS mechanism based up Eq. (12).

C. RLS RDR behavior as seen in Figs. 1 and 6

Potentially, one might hope to isolate the dominant RLS mechanism at low densities,[15] but this is not possible for reasons which will become clear. The most important of these is that the datas' uncertainty below 2 m/ℓ is simply too large. What is seen in Fig. 1 is a correlation via the same kinds of I/d vs d equations as found in Figs. 4 and 5 (see figure captions), i.e., $I/d=ad+bd^2+cd^3$. In all cases, i.e., Figs. 4 and 5 and Fig. 1, the quadratic ''ad'' term is large and positive, the cubic bd^2 term is between 0.1 and 0.05 of the ''ad'' term (and negative) and a very small ''cd^3'' quartic term (note that quadratic, cubic and quartic refer to the d in the denominator of I/d). The latter term is positive for I_{aniso} and negative for I_{iso}. Overall, the trend is expected at lower densities (predicting a zero value for $d=0$), but surprising at the higher densities due to the unexpected behavior of the dominate cross term from Eq. (12) for $l=0$ data. This data is generally consistent with the results of Ref. 3 for CF_4/Ar mixtures, but the details are clearly different, i.e., ν_1), the CF_4/Ar mixture using CF_4's ν_1 mode as a probe was done at much higher mole ratios of CF_4/Ar whereas our ratios are always 0.1 CH_4/CF_4. Perhaps more importantly, (2), the CF_4 does not have the large first and/or second Coriolis coupling constant (in fact, to the best of our knowledge the second order Coriolis constant is not reported) which disallows the $V-R$ correlation process and effectively eliminates the sensitivity that CH_4's ν_1 shows to density increases. The CF_4/Ar experiments were not done at high enough densities to observe three-body cancellation.

Figure 6 shows no evidence of the results seen by Posch for CCl_4,[15] or by us in CO_2.[19] We believe that this is to be expected because, unlike the Rayleigh light scattering results of Posch or our work on the dipole forbidden ν_2 mode of CO_2 (where, near W_0, the depolarization ratio is 3/4 and in the far wings 9/37). In the ν_1 of methane, there are no clear trends in the depolarization ratios. In particular, in CH_4's ν_1 we have I_{iso} with a large allowed component and I_{aniso} with a totally forbidden ν_1 component and no comparable RDR values to CCl_4[15] or to CO_2[19] can be seen in Fig. 6. The fact that Posch's results as well as ours, on CO_2, were gathered only from ii data and gave exactly the results predicted by Posch for CCl_4 and as we found for forbidden RLS signals of CO_2, we believe, confirms our assertion that one cannot use a ''mixed'' signal (allowed and forbidden) to assigned mechanisms. In CO_2, for example, the 3/4 RDR value near W_0 means that the DID mechanism occurs at longer times and the 9/37 RDR far wing (large $W-W_0$) values of the FGID mechanisms, occurs at shorter times. The results of Fig. 6, however, do not allow us access to most of the wing region that is expected to be dominated by ii effects. Thus a direct comparison with the RyLS results of CF_4 or CH_4 is not possible. This simply shows that this type of mechanistic test cannot be used for our CH_4 probe experiments. We again should note that a scan of duration approaching 9 h about ν_1 $W_0\pm50$ cm^{-1} showed no additional wing RLS.

VI. CONCLUSION

A Raman light scattering experiment as a function of density for a binary mixture of CH_4/CF_4 at mole ratio 0.1 was carried out using CH_4's ν_1 signal as a probe. Raman depolarization ratios were determined, but were shown not to

be useful for determining the scattering mechanism when plotted as a function of distance from the center of the allowed ν_1 CH_4 totally symmetric normal mode. The conclusions were as follows:

(1) The $I_{\rm iso}$ signal's origin arises from $V-R$ coupled vibrational dephasing via the second order Coriolis constant and ''turns-on'' the ⟨allowed-ii cross-term⟩ for the source of ii intensity in addition to the allowed ν_1 contribution.

(2) The origin of $I_{\nu h}=I_{\rm aniso}$ spectra is the usual DID and FGID mechanisms.

(3) $I_{\rm aniso}d$ vs d showed almost no signal cancellation and a simple lattice gas type of model showed this clearly (based on the work of Friederich, Tarjus, and Kivelson).

(4) A model (called the BL model) was given which elucidated the contributions of the two species (CH_4 an CF_4) to the observed RLS intensity for I_{zz} and I_{xz} (I_{vv} and I_{vh}) from v_1 methane.

(5) In principal, the BL model demonstrates the origin of both $I_{\rm aniso}$ and $I_{\rm iso}$ RLS signals by eliminating the assumption upon which other similar models are based. By eliminating the ''no $V-R$ correlation'' and given certain molecular properties, vibrational dephasing correlated with ii processes could become the dominant $I_{\rm iso}$ii RLS mechanism.

ACKNOWLEDGMENTS

The authors are indebted to many discussions with George Tabisz, Daniel Friend, and particularly with Harald Posch and Branka Ladanyi. The latter two workers contributed many hours of discussion and in Professor Ladanyi's case also the BL model for Raman light scattering from binary mixture systems. Ich bedanke mich! Lastly, this paper is dedicated to our fellow light scattering worker, Professor Heiner Versmold, to whom we wish a speedy recovery from his illness.

[1] *Phenomena Induced by Intermolecular Interactions*, edited by G. Birnbaum, NATO ASI Series (Plenum, New York, 1985).
[2] *Collision- and Interaction-Induced Spectroscopy*, edited by G. C. Tabisz and M. N. Neuman, NATO ASI Series C (Klewer, Dordrecht, 1995).
[3] Y. LeDuff, A. Gharbi, and T. Othman, Phys. Rev. A **28**, 2714 (1983).
[4] W. Holzer and Y. LeDuff, Phys. Rev. Lett. **32**, 205 (1974).
[5] Y. LeDuff and A. Gharbi, Phys. Rev. A **17**, 1729 (1978).
[6] M. Thibeau, A. Gharbi, Y. LeDuff, and V. Serviescu, J. Phys. (Paris) **38**, 641 (1977).
[7] E. J. Rose, E. Whitewolf, and F. G. Baglin, J. Chem. Phys. **97**, 4596 (1992), and see also F. G. Baglin, E. J. Rose, and S. Sweitzer, Mol. Phys. **84**, 115 (1994).
[8] A. D. Buckingham and A. J. C. Ladd, Can. J. Phys. **54**, 611 (1976).
[9] E. J. Rose and F. G. Baglin, Mol. Phys. **81**, 1049 (1994).
[10] M. Wright, T. Murphy, and F. G. Baglin, Mol. Phys. **82**, 277 (1994).
[11] E. J. Rose and F. G. Baglin, J. Raman Spectros. **25**, 791 (1994).
[12] A. D. Buckingham and G. C. Tabisz, Mol. Phys. **36**, 583 (1978).
[13] T. I. Cox and P. A. Madden, Mol. Phys. **43**, 287 (1981).
[14] J. H. Yoon, A. Hacura, and F. G. Baglin, J. Chem. Phys. **91**, 5230 (1989).
[15] H. A. Posch, Mol. Phys. **40**, 1137 (1980).
[16] A. Hacura, J. H. Yoon, and F. G. Baglin, J. Chem. Phys. **91**, 5218 (1989).
[17] D. Frenkel and J. P. McTague, J. Chem. Phys. **72**, 2801 (1980).
[18] P. A. Madden, in *Spectroscopy and Relaxation of Molecular Liquids*, edited by D. Steele and J. Yarwood (Elsevier, New York, 1991), pp. 140ff.
[19] A. Hacura, J. H. Yoon, and F. G. Baglin, J. Raman Spectros. **18**, 311 (1987).
[20] B. Ladanyi (unpublished results).
[21] D. P. Shelton and G. C. Tabisz, Mol. Phys. **40**, 299 (1980).
[22] H. A. Posch, Mol. Phys. **37**, 1059 (1979).
[23] G. Doege, R. Arndt, and J. Yarwood, Mol. Phys. **52**, 33 (1934).
[24] S. Bratos, in *Vibrational Spectroscopy of Molecular Liquids and Solids*, NATO ASI Series, **56**, 33 (1984).
[25] D. W. Oxtoby, *Adv. Chem. Phys. XL*, edited by I. Prigogine and S. A. Rice (Interscience, New York, 1979) p. 1.
[26] S. Bratos and G. Tarjus, Can. J. Chem. **63**, 2047 (1985).
[27] K. S. Schweitzer and D. Chandler, J. Chem. Phys. **76**, 2296 (1982).
[28] Dr. Daniel Friend at N.I.S.T. Thermophysics Division at Boulder should be consulted for details (dfriend@bldrdoc.gov) concerning the EOS simulation.
[29] D. R. Douslin, R. H. Harrison, and R. T. Moore, J. Chem. Phys. **71**, 3477 (1967).
[30] M. Thibeau, G. C. Tabisz, B. Oksengorn, and B. Vodar, J. Quant. Spectros. Radiate. Transfer **10**, 839 (1970).
[31] V. Friedrich, G. Tarjus, and D. Kivelson, J. Chem. Phys. **93**, 2246 (1990).
[32] C. Nakagawa and T. Shimanouchi, Spectrochim. Acta **181**, 513 (1962).
[33] J.-E. Lolk and A. Robiette, J. Mol. Spectros. **88**, 14 (1981).
[34] G. Doege and J. Yarwood, in *Spectroscopy and Relaxation of Molecular Liquids*, edited by D. Steele and J. Yarwood (Elsevier, New York, 1991), p. 247.
[35] P. C. M. Vam Woerkon, J. DeBleijser, M. DeZwart, and J. C. Leyte, Chem. Phys. **4**, 236 (1973).